

## Article

# Confined Spaces in Buildings with High Indoor Radon Concentration: A Case Study Analysis with the Application of Constructive Remediation Measures

Leonel J. R. Nunes  and António Curado \* 

proMetheus, Unidade de Investigação em Materiais, Energia e Ambiente para a Sustentabilidade, Instituto Politécnico de Viana do Castelo, Rua da Escola Industrial e Comercial de Nun'Alvares, 4900-347 Viana do Castelo, Portugal

\* Correspondence: [acurado@estg.ipvc.pt](mailto:acurado@estg.ipvc.pt)

**Abstract:** Radon is an increasingly common concern, mainly when it is found indoors exposing the users of the space to radiation. As a gas, radon is an element produced due to uranium decay; it emanates naturally from soil and is considered by the World Health Organization as the second most common cause of lung cancer. Several methodologies are available for mitigating the indoor radon concentration, with distinct improvements and efficiencies that need to be proved with on-site testing. The case study here presented analyzes the effect of applying a barrier membrane, covering the pavement of a ground floor room located in a historic building with a high occupancy rate, on an abnormal radon concentration evidenced by experimental data. After the barrier membrane installation, a new long-term monitoring campaign (3 months) was carried out to assess indoor radon concentration. The obtained results showed that the barrier membrane lowered the indoor radon concentration by 90%. However, the radon exposure level remained higher than the recommended level to enable safe occupation and the regular use of space. Nevertheless, as the reduction in the radon concentration was very significant by the adoption of a barrier membrane, the combination of this technical solution with other mitigation methodologies, namely including the adoption of mechanical ventilation procedures, can become a very efficient solution for radon remediation, reducing the number of air changes per hour (ACH) from 30–60 to 4–6.



**Citation:** Nunes, L.J.R.; Curado, A. Confined Spaces in Buildings with High Indoor Radon Concentration: A Case Study Analysis with the Application of Constructive Remediation Measures. *Buildings* **2023**, *13*, 49. <https://doi.org/10.3390/buildings13010049>

Academic Editor: Fani Antoniou

Received: 1 December 2022

Revised: 19 December 2022

Accepted: 21 December 2022

Published: 25 December 2022



**Copyright:** © 2022 by the authors. Licensee MDPI, Basel, Switzerland. This article is an open access article distributed under the terms and conditions of the Creative Commons Attribution (CC BY) license (<https://creativecommons.org/licenses/by/4.0/>).

**Keywords:** indoor radon concentration; mitigation measures; historical buildings retrofitting; radon barrier membranes

## 1. Introduction

Radon is a naturally occurring radioactive gas, with no color or smell; radon inhalation is the largest source of exposure to ionizing radiation in the population, contributing to more than 40% to the effective dose [1–4]. Prolonged exposure to indoor radon is the second leading cause of lung cancer, after tobacco, and the leading cause in non-smokers [5–7]. According to the literature, smokers and ex-smokers are at increased risk from the combined action of tobacco and radon [8]. However, there is no consistent evidence of a relationship between radon exposure and other types of cancer or disease [9–13]. Radon produces radioactive particles in the air people breathe, which are trapped in the airways and emit radiation that can cause lung damage, increasing the risk of lung cancer owing to prolonged exposures [14,15]. According to the World Health Organization (WHO), radon exposure is estimated to cause between 3% and 14% of lung cancers worldwide [16,17]. Across Europe, an estimated 9% of lung cancer deaths are due to radon exposure, accounting for around 2% of all cancer deaths [18,19].

Despite radon being everywhere, outside and inside buildings, certain areas are more prone to have high indoor radon levels [20,21]. Information about these areas can be obtained from radon susceptibility maps that are generally produced from wide-range

surveys based on extensive radon gas monitoring campaigns that are an indicator of the level of susceptibility to indoor radon [22,23]. Based on the evidence, it is consensually assumed that the only way to know the radon concentration is by measuring it [24,25].

Radon penetrates easily into enclosed spaces, such as the building's rooms, and can reach high indoor concentrations under some circumstances; the high concentrations can be aggravated with the reduction of natural ventilation through new window frames and shutter boxes, which result from rehabilitation works to improve energy efficiency, and are associated with the use of less gas permeable wall facades [26,27]. Additionally, there are frequent small cracks in buildings' floors and walls, formed due to causes related to differential foundations settlements, movements of thermal origin, or adjustments between construction elements, as well as some specific openings intentionally created for the passage of pipes and cables, and buildings expansion joints. The size and frequency of these cracks or gaps also depend on the finishing coat and the quality of construction [28–32]. These cracks are the path for radon to enter the building driven by the difference between atmospheric pressure within, which is generally lower than the pressure in the underlying ground [33,34]. In contrast, the temperature differences between the interior of the building (generally warmer) and the ground (usually cooler) result in a phenomenon commonly known as the chimney effect, and are effects of wind action [35].

The exposure to indoor radon can be reduced by implementing preventive measures in the construction phase of new buildings or through corrective or remediation measures for existing buildings [36–38]. The present work aims to analyze the effectiveness of the application of a radon barrier membrane on the floor of a compartment located in a historic building used as an academic building of a university institution, situated in a region with a granitic geological substrate, in which concentrations of indoor radon tend to be high. This building has limitations concerning interventions involving changes to the architectural nature, such as installing ducts for mechanical ventilation or opening windows, shutters, or other connections to the outside to promote natural or forced ventilation. In this way, the evaluation of the effectiveness of passive solutions of a constructive nature, as is the case of barrier membranes hidden under the floor, assumes a decisive role since it contributes to the reduction of the impact of other measures when it continues to be necessary to combine several methodologies to reduce the concentration of indoor radon.

## 2. Materials and methods

### 2.1. Framework

The Escola Superior Agrária de Ponte de Lima (ESA IPVC) is one of the six organizational units of the Instituto Politécnico de Viana do Castelo. The ESA IPVC campus is in the municipality of Ponte de Lima, in the parish of Refóios do Lima, in the Alto Minho region (Figure 1).

The ESA IPVC campus occupies approximately 17 hectares, distributed among agricultural production areas, animal production areas, experimental orchards, vineyards, olive groves, greenhouses, and academic buildings. Among the academic buildings, the main building, known as the Mosteiro de Refóios do Lima, stands out, which is classified as an architectural heritage and a national monument. For this reason, both the building and its surroundings have a set of restrictions regarding interventions of an architectural nature, or even recovery and rehabilitation.

Although there are few traces of the medieval period, the origins of the monastery building mostly date back to the twelfth century [39].

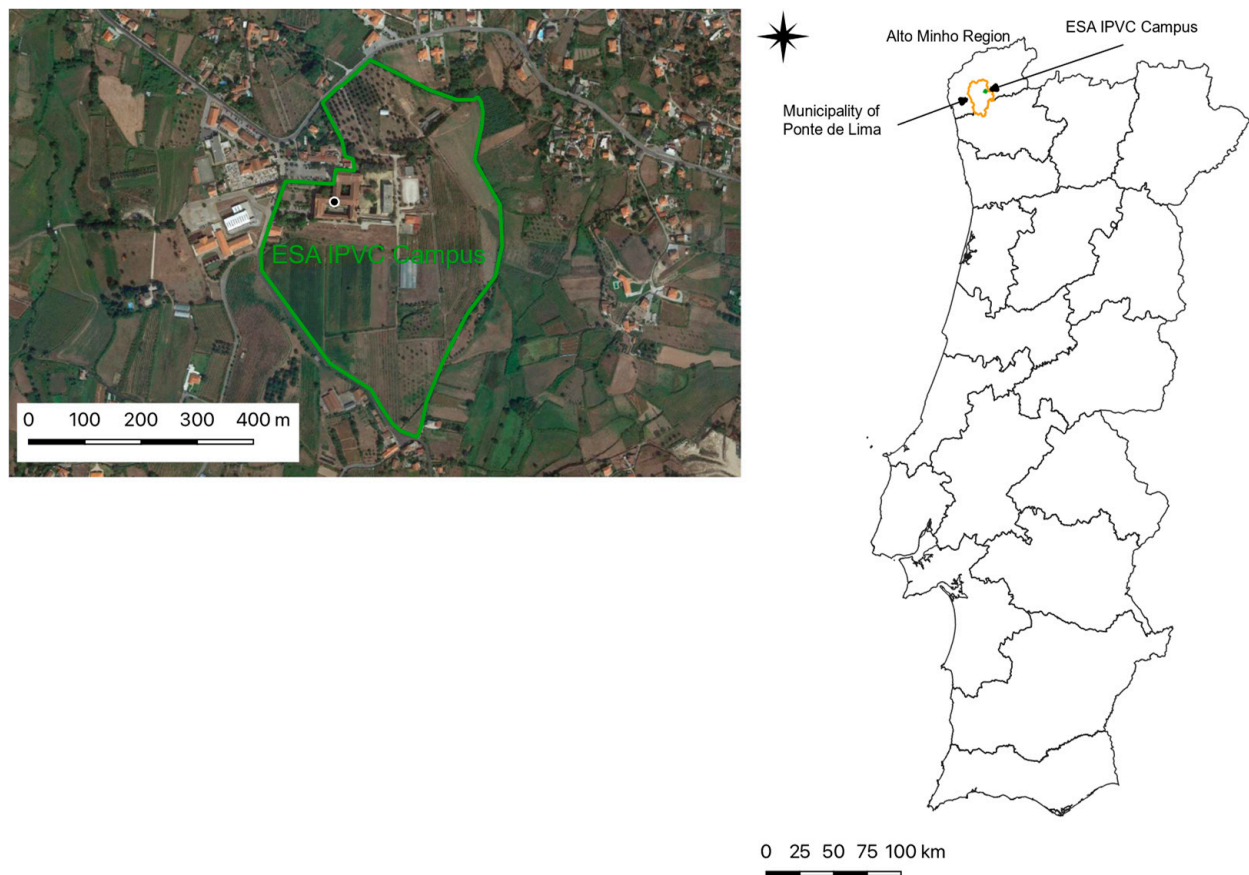


**Figure 1.** Location of the ESA IPVC campus. The dot on the building marks the position of the room where the indoor radon concentration measurements were taken.

However, the most brilliant construction took place between 1580 and 1810, with the beginning of the reconstruction of parts of the building, which should have been in ruins or at least extensively damaged. In 1770, the friars who inhabited the monastery were transferred to Mafra, by order of the Marquis of Pombal. The friars would eventually return to the monastery, where they continued to be involved in agricultural practice, which ended in 1834, with the extinction of religious orders in Portugal. After this period, the building passed into private ownership and began a long period of decay. In 1986, the building was acquired by the Municipality of Ponte de Lima, which began the recovery and rehabilitation of both the building, which was under the charge of the Architect Fernando Távora, and its surroundings, which were under the charge of the Landscape Architect Ilídio Alves Araújo. It was also during this period that the university institution was established in the building and the ESA IPVC campus was created. The main building is made up of two groups. The first group, from the second half of the 16th century, rests on primitive medieval foundations and includes a church, with the remaining structure built around a quadrangular central cloister. The second group, from the 18th century and later, has a set built around a patio, intended for agricultural tasks. The entire building is built in masonry, with granite serving as the main building material for the entire structure.

From a geological point of view, the region surrounding the ESA IPVC campus is made up of a relatively heterogeneous set of lithologies and structural features, as can be seen in Figure 2.

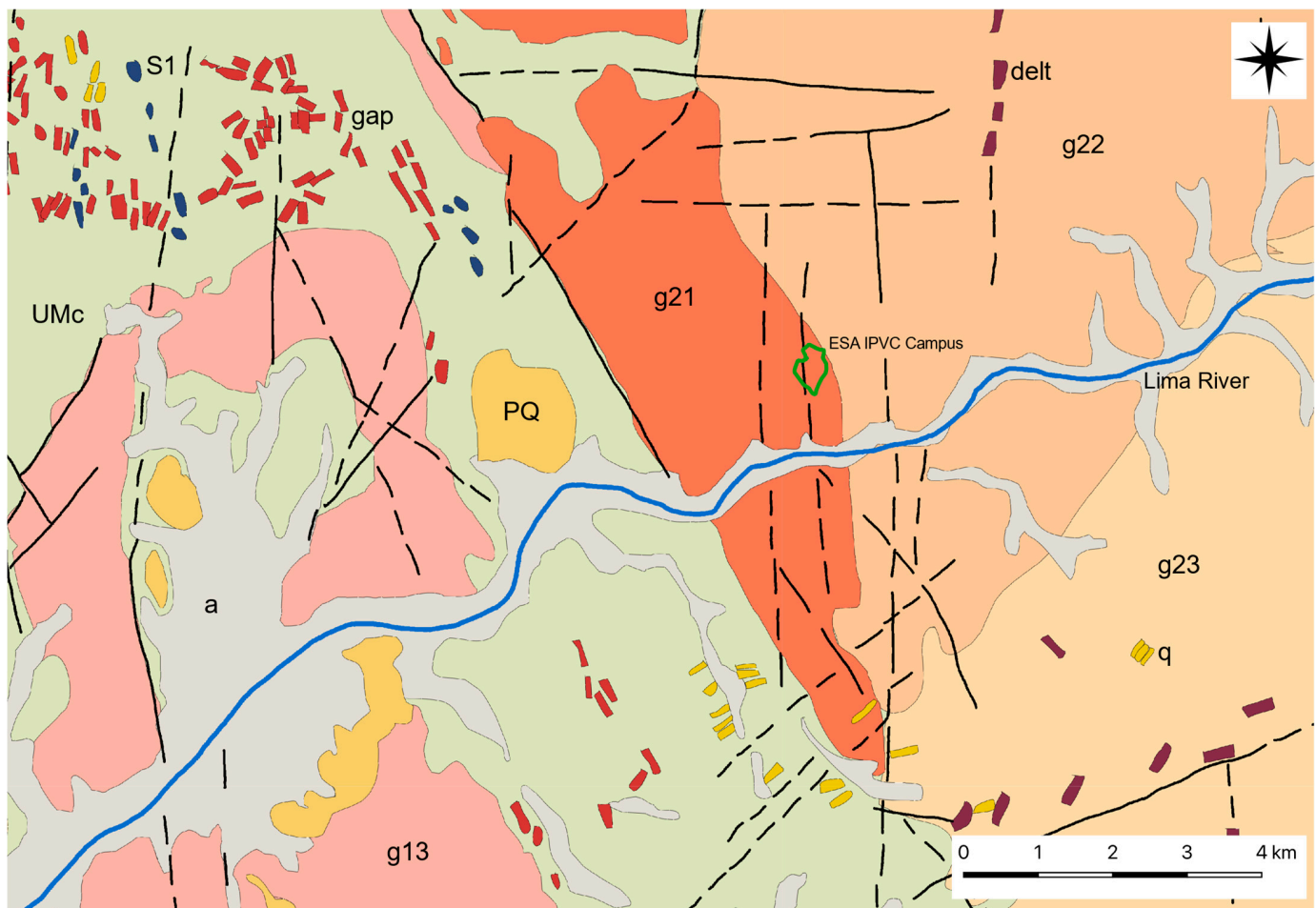


**Figure 2.** Geological framework of the Ponte de Lima region, where a—Fluvial and estuarine deposits, not current, accompany the channel of water courses, associated with current deposits; PQ—River and lake deposits are covered, or not, by periglacial solifluction deposits; g13—Medium-grained two-mica granite; g21—Porphyroid Granodiorite, biotitic, with highly developed megacrystals; g22—Porphyroid granite, coarse-grained, essentially biotitic; g23—Monzonitic granite, medium grain, porphyroid, with two micas, essentially biotitic; UMc—Pelites and psamites, skarns and vulcanites, black schists, gray quartzites and black schists with intercalations of ampelites and litites; S1—Phtanites, quartzites and black schists with intercalations of ampelites and litites; delt—Basic rocks; q—Quartz; and gap—Pegmatites and aplite-pegmatites (adapted from [40]).

The Lima River flows through this region, with an approximate orientation of ENE–WSW, and presents a predominance of granitoid rocks. The eastern sector presents lithologies associated with the Vigo–Régua ductile shear zone, where the clear separation caused by the structural accident (fault and probable fault), with NNW–SSE orientation, can be observed. In this eastern sector, extensive patches of coarse-grained porphyroid granite, essentially biotitic, occupy the northern part. Medium-grained, porphyroid, two-mica, essentially biotitic monzonitic granite occupies the southernmost part. In contact with the structural accident, there is also an important stain of biotitic porphyroid granodiorite, with highly developed megacrystals, completing the dominant group of syn-orogenic granites. In this eastern sector, there are also intrusions of masses and veins of quartz and basic rocks associated with structural accidents, but without reaching the frequency observed in the western sector of the area under analysis. The western sector is divided into two main groups, with medium-grained two-mica Hercynian granites occupying the central-south zone of this sector, surrounded by the parautochthonous Central Minho Unit, composed of pelites, psamites, and vulcanites, black schists, grey quartzites, and black schists with inter-



calations of ampelites and litites. The intrusion of quartz masses and veins, pegmatites, and aplite-pegmatites dots this western sector. There are also phthamites, quartzites, and black schists with intercalations of ampelites and litites from the group of carbonaceous schists of the Lower Silurian. The fluvial and lacustrine deposits covered or not, by periglacial solifluction deposits, from the early Quaternary and recent Pliocene, can be observed in some areas, mainly in the central-south region of the western sector, without occurring in the eastern sector. The fluvial and estuarine deposits (that do not accompany the channel of the rivers) are associated with current deposits from the Holocene to the actual period and are distributed by the two sectors, with a greater coverage in the western sector, associated with the enlargement of the bed of the river Lima.

Several structural accidents occur in the region under analysis, some of which are highlighted in Figure 3, with orientations tending to N–S and ENE–WSW, giving rise to blocks that move independently. These recent tectonic processes, probably of the Plio-Quaternary age, are of the compressive type and present with maximum stress in the E–W orientation.

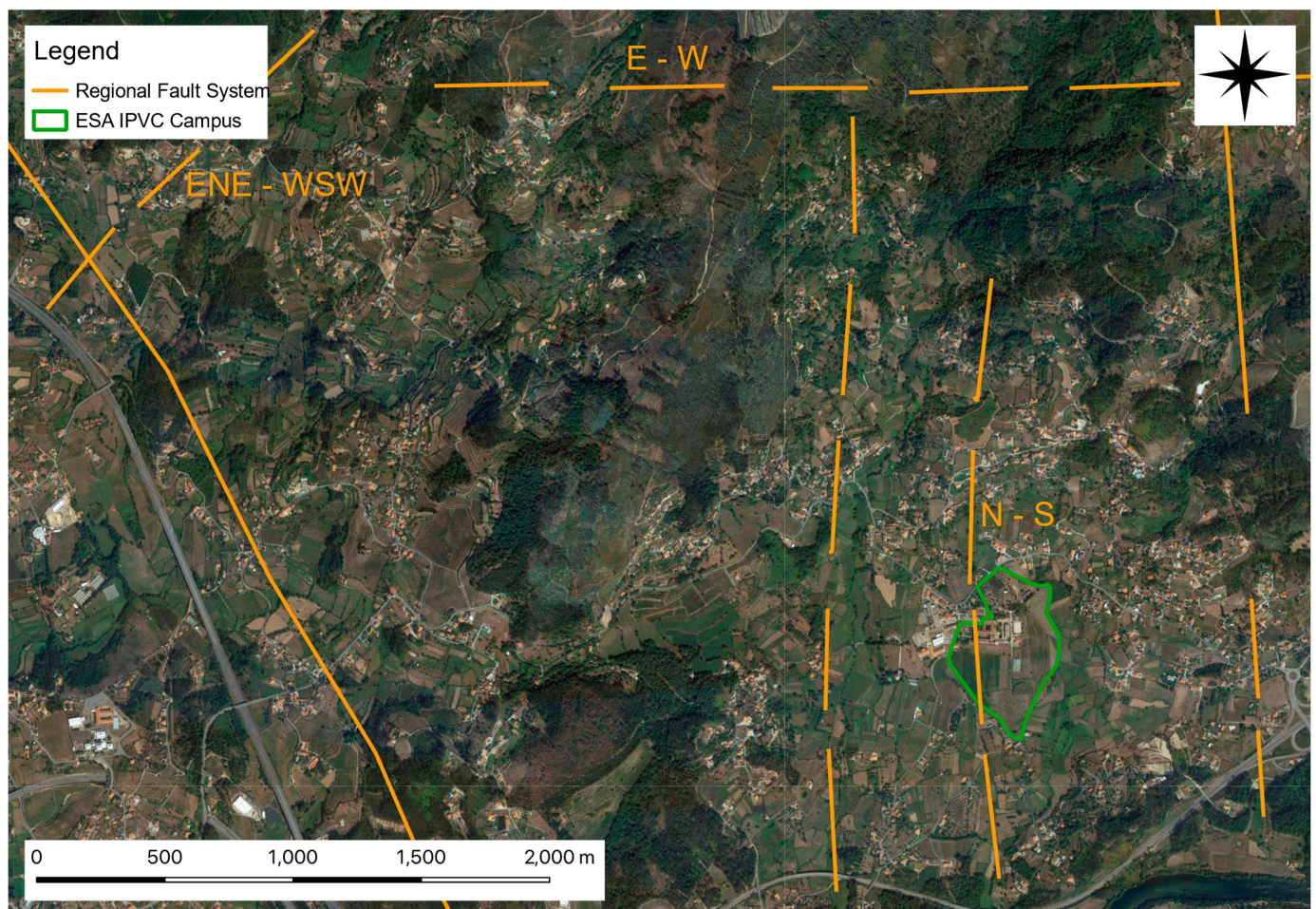


**Figure 3.** Scheme of the system of structural accidents that occur in the area under analysis, where fault systems and probable faults with N–S, ENE–WSW, and E–W orientation are identified (adapted from [40]).

This set of faults and probable faults, which create a mosaic of blocks with independent movements, together with the shear stress in the E–W direction cause a certain chaos in the structural set, which is extensively fractured. This situation may be the reason for the accumulation of indoor Rn; because if the lithological type that dominates the region is associated with a high structural discontinuity of rock massifs with high concentrations of

uranium, the Rn gas can more easily and quickly flow to the surface and emanate into the interior of buildings or the outside air following the radioactive decay of this element.

## 2.2. Monitoring and Data Acquisition

Abnormal concentrations of indoor Rn were detected in certain places of the main academic building through periodic monitoring carried out in the short-term mode (7 days), to prevent and avoid the exposure of users and visitors to the building to excessive Rn concentrations. Following this periodic monitoring, certain compartments, located in cellars, presented anomalous values, reaching concentrations of more than  $15,000 \text{ Bq}\cdot\text{m}^{-3}$  at certain peak moments. As these compartments were not being used for any specific purpose and did not have people inhabiting or visiting these components, it was decided to use these spaces as a testing area for the application of constructive remediation measures, such as the application of the barrier membranes.

In this sense, two campaigns were carried out to monitor the compartment. This compartment was located in the basement of the main academic building, with the floor (currently made of ceramic material) resting directly on the rock massif/ground. The compartment has an area of contact with the rocky substrate/soil of  $12.6 \text{ m}^2$  and a volume of  $34 \text{ m}^3$ . Monitoring was performed using two AirThings Corentium Plus Radon Monitor probes and a model QRI, and the technical specifications are shown in Table 1.

**Table 1.** Technical specifications of the AirThings Corentium Plus Radon Monitor probes and the model QRI, used in the different phases of monitoring the indoor Rn concentration.

Rn sampling	Passive diffusion chamber
Detection method	Alpha spectrometry
Detector	1 silicon photodiode
Diffusion time constant	25 min
Measurement range	$0\text{--}50,000 \text{ Bq}\cdot\text{m}^{-3}$
Sampling rate	1 h
	$4\text{ }^{\circ}\text{C}$ to $40\text{ }^{\circ}\text{C}$
Operation environment	5% RH to 85% RH non-condensing
	50 kPa to 110 kPa
Temperature	$0.336\text{ }^{\circ}\text{C}$ resolution, $\pm 1\text{ }^{\circ}\text{C}$ accuracy
Humidity	0.5% RH resolution, $\pm 4.5\%$ accuracy
Barometric pressure	0.01 kPa resolution, $\pm 1\text{ kPa}$ accuracy

Phase I monitoring was started on 13 March 2019 and was uninterruptedly performed until 13 June 2019, since the objective was to evaluate the Rn indoor concentration over a long-term period. After this period of monitoring, the Rn barrier membrane was applied. After completing this task, Phase II monitoring was carried out, which began on 3 September 2019 until 3 December 2019, according to the methodology that is outlined in Figure 4.

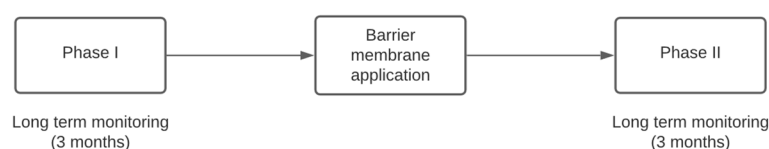


**Figure 4.** Temporal distribution of monitoring phases and other tasks.

## 3. Results and Discussion

The Rn concentration in the compartment was monitored using two probes, according to the procedure described above in Section 2.2. The measurement took place from 13 March 2019, starting at 5:23 pm, until 13 June 2019, ending at 4:23 pm, with 2181 measurements being obtained on each probe. Then, the data obtained in each of the probes were compared, to verify if there were significant differences between the two sets of data. For this purpose,



the averages and variances of the two data groups were compared through the t-Student and F-Snedecor tests. In both situations,  $p$ -values greater than 0.5 were obtained, i.e., in both situations, the null hypothesis ( $H_0$ ) was not rejected, which means that there were no significant differences between the averages or variances of the two groups; the variances were supposedly equal. Thus, it was understood that it is possible to transform the two groups of data into one, by calculating the average of the two groups. The results obtained are summarized in Table 2.

**Table 2.** Summarized data obtained from the initial monitoring of Rn concentration, carried out from 13 March 2019 to 13 June 2019.

Monitoring Period	13 March 2019–13 June 2019
No. of measurements	2181
Average value	6479.6 Bq·m <sup>-3</sup>
Standard deviation	3900.8 Bq·m <sup>-3</sup>
Max. value	18,737.7 Bq·m <sup>-3</sup>
Min. value	134.2 Bq·m <sup>-3</sup>

As can be seen using the long-term data obtained (3 months), the results show extremely high values, ranging between 134.2 Bq·m<sup>-3</sup> and 18,737.7 Bq·m<sup>-3</sup>, indicating a high standard deviation (3900.8 Bq·m<sup>-3</sup>) around the mean value (6479.6 Bq·m<sup>-3</sup>). As the objective was to stabilize the concentration of Rn at values below 300 Bq·m<sup>-3</sup>, we proceeded to distribute the obtained results in intervals of occurrence of 300 Bq·m<sup>-3</sup> to be able to analyze the occurrence of the different values of Rn concentration throughout the analysis, as shown in Figure 5.

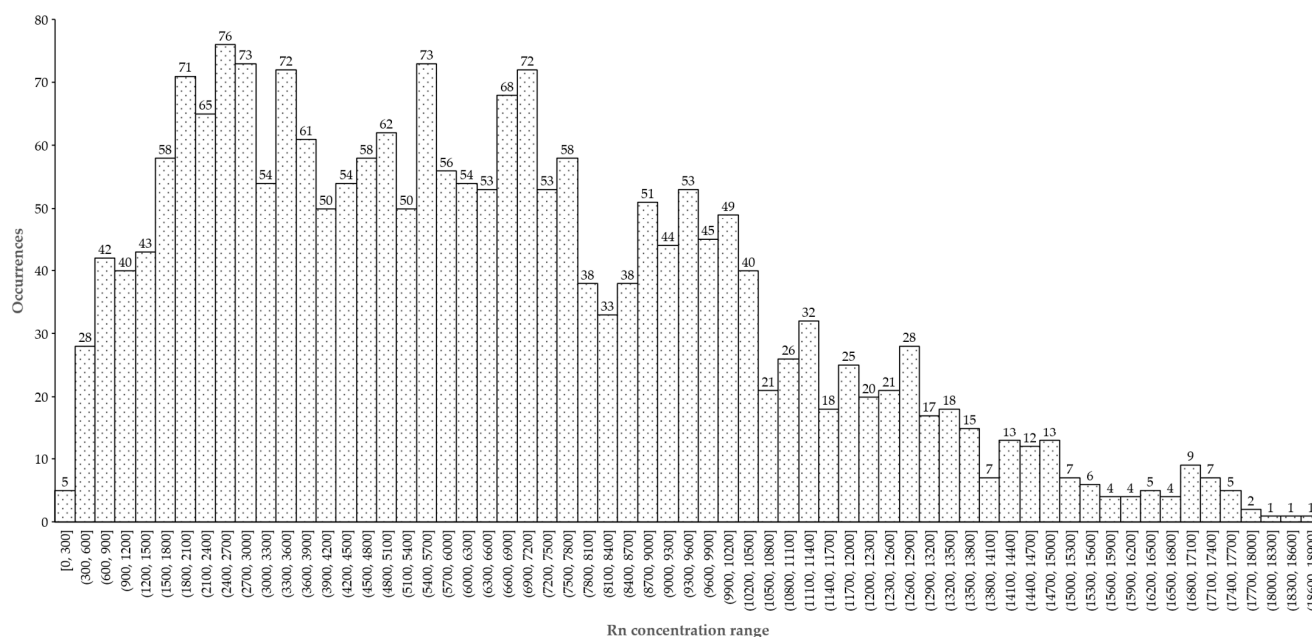


**Figure 5.** Distribution of results obtained in monitoring the Rn concentration by frequency intervals.

As can be seen from the distribution of the results, only five occurrences fall within the interval [0, 300] Bq·m<sup>-3</sup>, corresponding to 0.2% of all measurements performed. In contrast, in the interval [300, 10,200] Bq·m<sup>-3</sup>, there were 1891 occurrences, which correspond to 86.7% of the results obtained. In the interval [10,200, 18,900] Bq·m<sup>-3</sup>, 285 results were included, corresponding to 13.1% of the total occurrences.

The results indicate the formation of a harmful environment in this space which, if intended for human use, would imply the need for 30–60 air renovations per hour (NR·h<sup>-1</sup>) (Annex VI of Decree-Law No. 79/2006, of 4 April, available at <https://files.dre.pt/1s/2006/04/067a00/>

[24162468.pdf](#), accessed on 10 October 2022). In other words, given that the compartment has a volume of  $34 \text{ m}^3$ , it would be necessary to extract  $1020\text{--}2040 \text{ m}^3 \cdot \text{h}^{-1}$ .

Given the high volume of air that would have to be renewed every hour, it was decided to use a constructive remediation solution, with the application of a barrier membrane. In this case, an Rn barrier membrane Monarflex RMB350, from Necoflex was applied. It is a membrane made from blends of virgin low-density polyethylene, with the specifications shown in Table 3.

**Table 3.** Technical specifications of Monarflex RMB350 (<http://www.necoflex.is>, accessed on 10 October 2022).

Elongation	19%
Tear resistance	405 N
Water vapor transmission	$0.03 \text{ g} \cdot \text{m}^{-2} \cdot \text{d}^{-1}$
Color tone	Red (top side) and black (underside)
Thickness	0.35 mm

Figure 6 shows the initial state of the compartment floor and its appearance after the placement of the Rn barrier membrane. As can be seen in Figure 6b, it is important to finish at the base of the wall, to avoid points where Rn can cross owing to the bad placement of the mesh.



**Figure 6.** Placement of the Rn barrier membrane. (a) Floor before placing the barrier membrane; (b) Floor after placing the barrier membrane.

After placing the Rn barrier membrane, new monitoring was carried out. This monitoring was also carried out with two probes, according to the procedure described in Section 2.2, starting on 3 September 2019, at 5:49 pm, and ending on 3 December 2019, at 1:49 pm. In this monitoring campaign, in which two probes were also used, the data obtained were compared using the same methods used for the pre-application campaign of the barrier membrane. The results obtained with the t-Student and F-Snedecor tests were always higher than 0.5, not rejecting the null hypothesis ( $H_0$ ). Thus, there were no significant differences between the means of the two data groups, as well as between the presented variances, which are supposedly equal. These results validated the procedure of merging the two groups of data and using the average value.

Figure 7 shows the superposition of the results of monitoring the Rn concentration before and after the application of the barrier membrane.



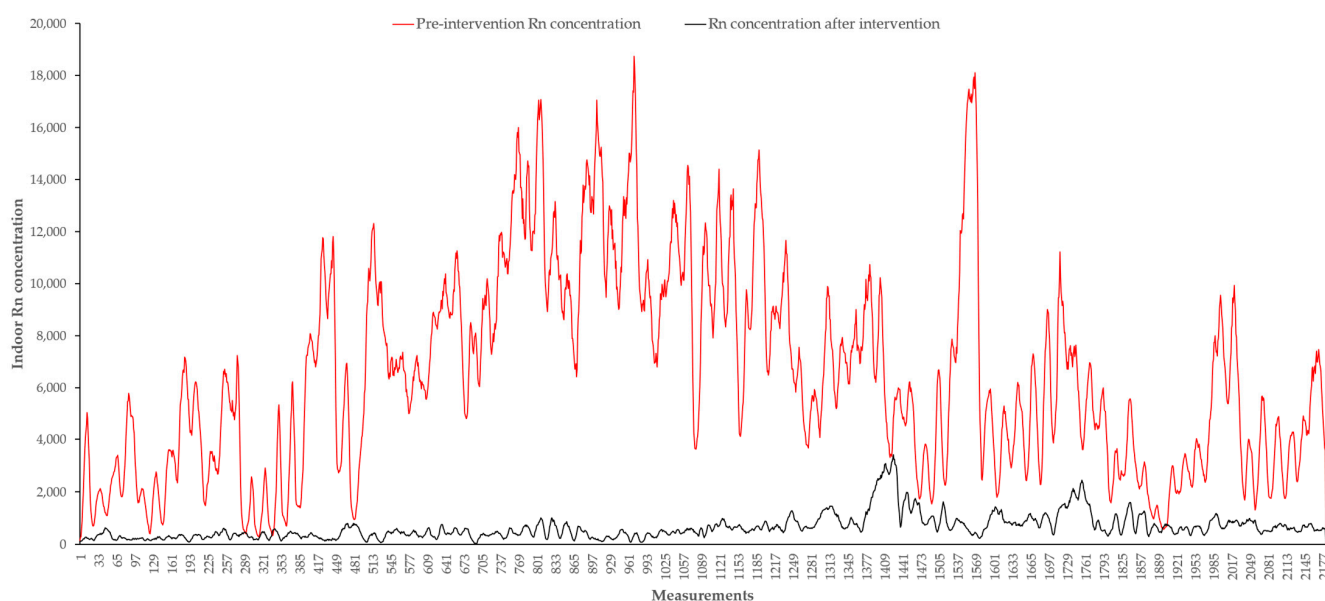


**Figure 7.** Results obtained before and after the application of the barrier membrane.

As can be seen, the difference between the results obtained in the two monitoring campaigns was significant. The results obtained in the post-application campaign are summarized in Table 4.

**Table 4.** Data obtained from monitoring the concentration of Rn after the application of the barrier membrane, carried out from 3 September 2019 to 3 September 2019.

Monitoring Period	3 September 2019–3 September 2019
No. of measurements	2181
Average value	634.4 Bq·m <sup>−3</sup>
Standard deviation	475.0 Bq·m <sup>−3</sup>
Max. value	3407.4 Bq·m <sup>−3</sup>
Min. value	21.7 Bq·m <sup>−3</sup>

Next, the results obtained were distributed by the classes of Rn concentration, for successive intervals of 300 Bq·m<sup>−3</sup>, as shown in Figure 8.

The application of the barrier membrane caused a 90% reduction in the average values measured in the pre-intervention and post-intervention monitoring campaigns. However, as can be seen in the results presented in Figure 4, only 452 occurrences, corresponding to 20.7% of the measurements, were recorded in the interval [0, 300] Bq·m<sup>−3</sup>. In other words, 79.3% of the measurements continued to record values above 300 Bq·m<sup>−3</sup>. However, only 48 occurrences were recorded in the concentration range [2100, 3600] Bq·m<sup>−3</sup>, corresponding to 2.2% of the total measurements, indicating the effectiveness of the barrier membrane in reducing the concentration of Rn. Thus, correction using a mechanical extraction system seems plausible considering the nature of the place (following the same legal document mentioned above), which could now be considered a cellar or a garage, with 4–6 NR·h<sup>−1</sup>, and the flow to be extracted would be 136–204 m<sup>3</sup>·h<sup>−1</sup>.

Previous references have suggested the use of barrier membranes to reach an acceptable radon level, for example, the work presented by Rasmussen and Cornelius [41]. They used an adequate radon concentration of 100 Bq·m<sup>−3</sup> in indoor air with several higher radon levels to evaluate the different radon barriers to prevent air penetration from the ground. In the current study, as the concentrations used were considerably lower, the barrier membranes used were almost entirely effective. The situation described in the current ESA IPVC case study is completely different because it is impossible to consider that the

barrier membrane used can have a definitive effect on the indoor radon concentration of the compartment. As seen in the results presented in the previous section, the indoor radon concentration measured in the compartment after applying the barrier membrane dropped significantly. However, despite this decrease in the indoor radon concentration, it still presents values well above the limit that can be considered acceptable, as it continues to be above  $300 \text{ Bq}\cdot\text{m}^{-3}$  during a significant part of the period in which the monitoring occurred.

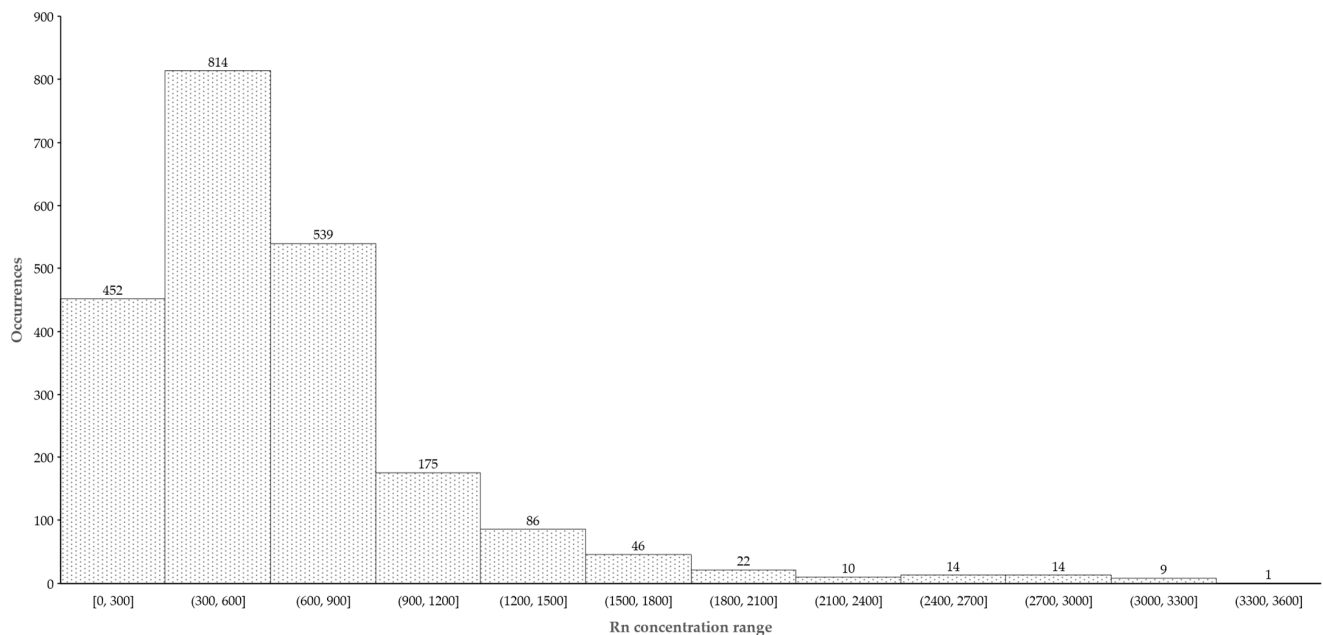


**Figure 8.** Distribution of the results obtained after monitoring the Rn concentration considering the frequency intervals.

Although in the current case study by ESA IPVC, the result is not entirely satisfactory, the situation may be related to other factors, as presented by Jelle et al. [42], including the fact that radon transport into buildings might be dominated by diffusion, pressure-driven flow, or something in between depending on the current values of the various parameters. These authors conclude that, from the results they obtained, most radon transport from the building ground to the indoor air is due to air leakage driven by pressure differences through the construction.

Thus, in the specific situation of the current ESA IPVC case study, the measured values continue to represent a problem. However, as demonstrated previously, with the application of the barrier membrane, the indoor radon concentration reached a result that can already be mitigated using active methods, namely, through mechanical ventilation. Despite this possibility and considering the conclusions of the study conducted by Jelle et al. [42], it is convenient to ensure that there is no circulation of radon gas through the building, as the pressure differences may be driving air with high concentrations of radon to the compartment. Thus, despite the high efficiency of the barrier membrane in blocking the transport of radon from the ground to the indoor air, it may be necessary to replicate the process on the entire floor of the building in direct contact with the ground for the measure to be fully efficient; this will help avoid the accumulation of high radon concentrations in other compartments, which later migrate and uniformize the concentration of radon throughout the floor.

#### 4. Conclusions

Radon gas is a radioactive gas that naturally occurs owing to the decay of uranium. When released into the atmosphere, radon poses no threat whatsoever. However, when released into buildings, radon can become concentrated, posing a risk to occupants and users of the space who may be exposed to high radon concentrations. Several mitigation processes are already available to counteract the gas concentration inside buildings. The effectiveness of each of the existing measures depends significantly on the starting point and combining more than one solution is often necessary. As demonstrated by the case study analyzed in the present work, using barrier membranes, even in extreme situations with very high indoor radon concentrations, can significantly reduce radon concentration. Despite a reduction of approximately 90% of the initial concentration, the monitoring carried out after the barrier membrane application still shows a radon concentration above the recommended values considering the presence of users. However, using a mechanical ventilation system becomes much more feasible than using a barrier membrane considering that the number of air changes per hour is considerably lower. These issues are of increasing importance, because, in addition to the concern with the safety of building users, the concern with energy efficiency becomes increasingly urgent as a pillar of the management of service buildings, as is the case of the academic building of ESA IPVC.

**Author Contributions:** Conceptualization, L.J.R.N. and A.C.; methodology, L.J.R.N. and A.C.; validation, L.J.R.N. and A.C.; formal analysis, L.J.R.N. and A.C.; investigation, L.J.R.N. and A.C.; resources, L.J.R.N. and A.C.; data curation, L.J.R.N. and A.C.; writing—original draft preparation, L.J.R.N. and A.C.; writing—review and editing, L.J.R.N. and A.C.; visualization, L.J.R.N. and A.C.; supervision, L.J.R.N. and A.C. All authors have read and agreed to the published version of the manuscript.

**Funding:** L.J.R.N. was supported by proMetheus, Research Unit on Energy, Materials and Environment for Sustainability—UIDP/05975/2020, funded by national funds through FCT—Fundação para a Ciência e Tecnologia. A.C. co-authored this work within the scope of the project proMetheus, Research Unit on Materials, Energy, and Environment for Sustainability, FCT Ref. UID/05975/2020, financed by national funds through the FCT/MCTES.

**Data Availability Statement:** The data are available upon request to the corresponding author.

**Acknowledgments:** The authors thank Óscar Ribeiro da Silva, from RADÃO STOP, for providing the radon barrier membrane used in this study.

**Conflicts of Interest:** The authors declare no conflict of interest.

#### References

1. UNSCEAR. *United Nations Scientific Committee on the Effects of Atomic Radiation UNSCEAR 2008—Report to the General Assembly with Scientific Annexes: Sources and Effects of Ionizing Radiation*; United Nations Scientific Committee on the Effects of Atomic Radiation: New York, NY, USA, 2010.
2. Stoulos, S.; Manolopoulou, M.; Papastefanou, C. Assessment of Natural Radiation Exposure and Radon Exhalation from Building Materials in Greece. *J. Environ. Radioact.* **2003**, *69*, 225–240. [[CrossRef](#)] [[PubMed](#)]
3. Protection against Radon-222 at Home and at Work. A Report of a Task Group of the International Commission on Radiological Protection. *Ann. ICRP* **1993**, *23*, 1–45.
4. Nazaroff, W.W. Radon Transport from Soil to Air. *Rev. Geophys.* **1992**, *30*, 137–160. [[CrossRef](#)]
5. Samet, J.M.; Eradze, G.R. Radon and Lung Cancer Risk: Taking Stock at the Millenium. *Environ. Health Perspect.* **2000**, *108*, 635–641. [[CrossRef](#)] [[PubMed](#)]
6. Al-Zoughool, M.; Krewski, D. Health Effects of Radon: A Review of the Literature. *Int. J. Radiat. Biol.* **2009**, *85*, 57–69. [[CrossRef](#)] [[PubMed](#)]
7. Darby, S.; Hill, D.; Auvinen, A.; Barros-Dios, J.M.; Baysson, H.; Bochicchio, F.; Deo, H.; Falk, R.; Forastiere, F.; Hakama, M.; et al. Radon in Homes and Risk of Lung Cancer: Collaborative Analysis of Individual Data from 13 European Case-Control Studies. *BMJ* **2005**, *330*, 223. [[CrossRef](#)] [[PubMed](#)]
8. Hahn, E.J.; Rademacher, K.; Wiggins, A.; Rayens, M.K. Personalized Report-Back to Renters on Radon and Tobacco Smoke Exposure. *J. Environ. Health* **2018**, *80*, 8–14.
9. Lemjabbar-Alaoui, H.; Hassan, O.U.I.; Yang, Y.W.; Buchanan, P. Lung Cancer: Biology and Treatment Options. *Biochim. Biophys. Acta Rev. Cancer* **2015**, *1856*, 189–210. [[CrossRef](#)]

10. Krewski, D.; Lubin, J.H.; Zielinski, J.M.; Alavanja, M.; Catalan, V.S.; Field, R.W.; Klotz, J.B.; L  tourneau, E.G.; Lynch, C.F.; Lyon, J.I.; et al. Residential Radon and Risk of Lung Cancer: A Combined Analysis of 7 North American Case-Control Studies. *Epidemiology* **2005**, *16*, 137–145. [[CrossRef](#)]
11. Alberg, A.J.; Ford, J.G.; Samet, J.M. Epidemiology of Lung Cancer: ACCP Evidence-Based Clinical Practice Guidelines (2nd Edition). *Chest* **2007**, *132*, 29S–55S. [[CrossRef](#)]
12. Subramanian, J.; Govindan, R. Lung Cancer in Never Smokers: A Review. *J. Clin. Oncol.* **2007**, *25*, 561–570. [[CrossRef](#)] [[PubMed](#)]
13. Baltrenas, P.; Grubliauskas, R.; Danila, V. Seasonal Variation of Indoor Radon Concentration Levels in Different Premises of a University Building. *Sustainability* **2020**, *12*, 6174. [[CrossRef](#)]
14. Sharma, N.; Singh, J.; Kaur, B. Performance Study of Some Reverse Osmosis Systems for Removal of Uranium and Total Dissolved Solids in Underground Waters of Punjab State, India. *J. Adv. Phys.* **2014**, *4*, 123–132. [[CrossRef](#)]
15. Yang, S.; Pernot, J.G.; J  rin, C.H.; Niculita-Hirzel, H.; Perret, V.; Licina, D. Energy, Indoor Air Quality, Occupant Behavior, Self-Reported Symptoms and Satisfaction in Energy-Efficient Dwellings in Switzerland. *Build. Environ.* **2020**, *171*, 106618. [[CrossRef](#)]
16. WHO. *WHO Handbook on Indoor Radon: A Public Health Perspective*; World Health Organization: Geneva, Switzerland, 2009.
17. Bossew, P.; Cinelli, G.; Ciotoli, G.; Crowley, Q.G.; de Cort, M.; Medina, J.E.; Gruber, V.; Petermann, E.; Tollefsen, T. Development of a Geogenic Radon Hazard Index—Concept, History, Experiences. *Int. J. Environ. Res. Public Health* **2020**, *17*, 4134. [[CrossRef](#)]
18. Tracy, B.L.; Krewski, D.; Chen, J.; Zielinski, J.M.; Brand, K.P.; Meyerhof, D. Assessment and management of residential radon health risks: A report from the health Canada radon workshop. *J. Toxicol. Environ. Health Part A* **2006**, *69*, 735–758. [[CrossRef](#)]
19. Figueiredo, A.; Ferreira, C.; Ulisses, P.; M  rquez-Medina, D. Lung Cancer Overview. In *Fighting Lung Cancer with Conventional Therapies*; Nova Science Publishers, Inc.: New York, NY, USA, 2015.
20. Lugg, A.; Probert, D. Indoor Radon Gas: A Potential Health Hazard Resulting from Implementing Energy-Efficiency Measures. *Appl. Energy* **1997**, *56*, 93–196. [[CrossRef](#)]
21. Ahmad, N.; Uddin, Z.; Rehman, J.U.; Bakhsh, M.; Ullah, H. Evaluation of Radon Concentration and Heavy Metals in Drinking Water and Their Health Implications to the Population of Quetta, Balochistan, Pakistan. *Int. J. Environ. Anal. Chem.* **2020**, *100*, 32–41. [[CrossRef](#)]
22. Royse, K.R. The Handling of Hazard Data on a National Scale: A Case Study from the British Geological Survey. *Surv. Geophys.* **2011**, *32*, 753–776. [[CrossRef](#)]
23. Fisk, W.J.; Singer, B.C.; Chan, W.R. Association of Residential Energy Efficiency Retrofits with Indoor Environmental Quality, Comfort, and Health: A Review of Empirical Data. *Build. Environ.* **2020**, *180*, 107067. [[CrossRef](#)]
24. Moore, W.S. Fifteen Years Experience in Measuring 224Ra and 223Ra by Delayed-Coincidence Counting. *Mar. Chem.* **2008**, *109*, 188–197. [[CrossRef](#)]
25. Adelikhah, M.; Shahrokhi, A.; Imani, M.; Chalupnik, S.; Kov  cs, T. Radiological Assessment of Indoor Radon and Thoron Concentrations and Indoor Radon Map of Dwellings in Mashhad, Iran. *Int. J. Environ. Res. Public Health* **2021**, *18*, 141. [[CrossRef](#)] [[PubMed](#)]
26. Samuelsson, C. Retrospective Determination of Radon in Houses. *Nature* **1988**, *334*, 338–340. [[CrossRef](#)] [[PubMed](#)]
27. Sabbarese, C.; Ambrosino, F.; D’Onofrio, A. Development of Radon Transport Model in Different Types of Dwellings to Assess Indoor Activity Concentration. *J. Environ. Radioact.* **2021**, *227*, 106501. [[CrossRef](#)] [[PubMed](#)]
28. Paridaens, J.; de Saint-Georges, L.; Vanmarcke, H. Mitigation of a Radon-Rich Belgian Dwelling Using Active Subslab Depressurization. *J. Environ. Radioact.* **2005**, *79*, 25–37. [[CrossRef](#)]
29. G  czi, G.; Ben  cs, J.; Krist  f, K.; Horv  th, M. High Concentrations of Radon and Carbon Dioxide in Energy-Efficient Family Houses without Heat Recovery Ventilation. *J. Environ. Eng. Landsc. Manag.* **2018**, *26*, 64–74. [[CrossRef](#)]
30. Tan, Y.; Yuan, H.; Kearfott, K. A Model Comparison of Diffusion-Controlled Radon Exhalation from Solid and Cavity Walls with Application to High Background Radiation Areas. *Environ. Sci. Pollut. Res.* **2020**, *27*, 43389–43395. [[CrossRef](#)]
31. Frutos-Puerto, S.; Pinilla-Gil, E.; Andrade, E.; Reis, M.; Madruga, M.J.; Rodr  guez, C.M. Radon and Thoron Exhalation Rate, Emanation Factor and Radioactivity Risks of Building Materials of the Iberian Peninsula. *PeerJ* **2020**, *8*, e10331. [[CrossRef](#)]
32. Park, J.H.; Lee, C.M.; Kang, D.R. A Deterministic Model for Estimating Indoor Radon Concentrations in South Korea. *Int. J. Environ. Res. Public Health* **2019**, *16*, 3424. [[CrossRef](#)]
33. Wang, F.; Ward, I.C. Modelling Multiple Radon Entry and Transport in a Domestic Dwelling. *Build. Environ.* **1997**, *32*, 341–350. [[CrossRef](#)]
34. Wang, F.; Ward, I.C. Multiple Radon Entry Modeling in a House with a Cellar. *J. Air Waste Manag. Assoc.* **1999**, *49*, 682–693. [[CrossRef](#)]
35. Mehdipour, L.A.; Mortazavi, S.M.J.; Saion, E.B.; Mozdarani, H.; Aziz, S.A.; Kamari, H.M.; Faghihi, R.; Mehdizadeh, S.; Kardan, M.R.; Mortazavi, A.; et al. Natural Ventilation Considerations for Radon Prone Areas of Ramsar. *Int. J. Radiat. Res.* **2014**, *12*, 69–74.
36. Henschel, D.B. Analysis of Radon Mitigation Techniques Used in Existing Us Houses. *Radiat. Prot. Dosim.* **1994**, *56*, 21–27. [[CrossRef](#)]
37. Groves-Kirkby, C.J.; Denman, A.R.; Phillips, P.S.; Crockett, R.G.M.; Woolridge, A.C.; Tornberg, R. Radon Mitigation in Domestic Properties and Its Health Implications—a Comparison between during-Construction and Post-Construction Radon Reduction. *Environ. Int.* **2006**, *32*, 435–443. [[CrossRef](#)]



38. Khan, S.M.; Gomes, J.; Krewski, D.R. Radon Interventions around the Globe: A Systematic Review. *Heliyon* **2019**, *5*, e01737. [[CrossRef](#)]
39. Valin, I.; Rodrigues, A.C.; Brito, L. *Miguel De Mosteiro a Escola: ESA IPVC 35o Aniversário*; Oficina das Edições: Ponte de Lima, Portugal, 2021.
40. *Carta Geológica De Portugal, Escala 1/200000—Notícia Explicativa Da Folha 1*; Pereira, E. (Ed.) Serviços Geológicos de Portugal: Lisbon, Portugal, 1993.
41. Valdbjørn Rasmussen, T.; Cornelius, T. Use of Radon Barriers to Reach an Acceptable Radon Level. In Proceedings of the E3S Web of Conferences, Tallinn, Estonia, 6–9 September 2020; Volume 172.
42. Jelle, B.P.; Noreng, K.; Erichsen, T.H.; Strand, T. Implementation of Radon Barriers, Model Development and Calculation of Radon Concentration in Indoor Air. *J. Build. Phys.* **2011**, *34*, 195–222. [[CrossRef](#)]

**Disclaimer/Publisher’s Note:** The statements, opinions and data contained in all publications are solely those of the individual author(s) and contributor(s) and not of MDPI and/or the editor(s). MDPI and/or the editor(s) disclaim responsibility for any injury to people or property resulting from any ideas, methods, instructions or products referred to in the content.